*Journal of Organometallic Chemistry*, 383 (1990) 279–294
Elsevier Sequoia S.A., Lausanne – Printed in The Netherlands
JOM 20266

# Chemistry of carbonyl-derived ligands. Nucleophilic attack on anionic acetylide clusters

**Michael P. Jensen, Michal Sabat, Dean H. Johnston, Lisa M. Jones and Duward F. Shriver** *

*Department of Chemistry, Northwestern University, Evanston, Il 60208 (U.S.A.)*

Received April 21st, 1989)

## Abstract

The broad range of reactions of anionic ketenylidene clusters is reviewed. We then describe some chemistry of the triiron nonacarbonyl acetylide clusters (PPN)[$Fe_3(CO)_9CCOR$] (Ia,Ib), (a: R = $CH_2CH_3$; b: R = $C(O)CH_3$; PPN = bis(triphenylphosphine)iminium (1 +), $(Ph_3P)_2N^+$), which are derived from the iron ketenylidene $(PPN)_2[Fe_3(CO)_9CCO]$. The ethoxyacetylide cluster Ia adds a single phosphine to form a phosphonium alkyne (PPN)[$Fe_3(CO)_9PMePh_2CCOEt$] (II). In contrast, Ib reacts with loss of acetate anion to form an unusual phosphonium acetylide cluster [$Fe_3(CO)_9CCPMePh_2$] (III), which is also formed cleanly by protonation of II with one equivalent of triflic acid, $HSO_3CF_3$. Implications of the formation of these products on bonding and mechanism are considered. Clusters II and III are spectroscopically characterized, and a single crystal X-ray structure determination of II and III are reported.

(PPN)[$Fe_3(CO)_9PMePh_2CCOEt$] (II) crystallizes in the triclinic space group $P\bar{1}$; *a* 9.910(1); *b* 16.920(2); *c* 17.372(2) Å; $\alpha$ 74.83(1)°; $\beta$ 84.65(1)°; $\gamma$ 86.07(1)°; *V* 2796(1) Å$^3$; *Z* = 2. [$Fe_3(CO)_9CCPMePh_2$] (III) crystallizes with an orthorhombic lattice; space group *Pbca*; *a* 7.898(1); *b* 19.885(2); *c* 31.906(5) Å; *V* 5011(2) Å$^3$; *Z* = 8.

## Introduction

The iron ketenylidene, $(PPN)_2[Fe_3(CO)_9CCO]$, is derived from $(PPN)_2[Fe_3(CO)_{11}]$, eq. 1. [1]. The ketenylidene ligand, CCO, is an example of a cluster-

$$[Fe_3(CO)_{11}]^{2-} \xrightarrow{AcCl} \xrightarrow[-OAc^-]{2e^-} [Fe_3(CO)_9CCO]^{2-} \quad (1)$$

stabilized ligand derived entirely from terminal carbonyls. This ligand readily undergoes a wide variety of reactions [2] to yield many new products (Scheme 1).

0022-328X/90/$03.50 

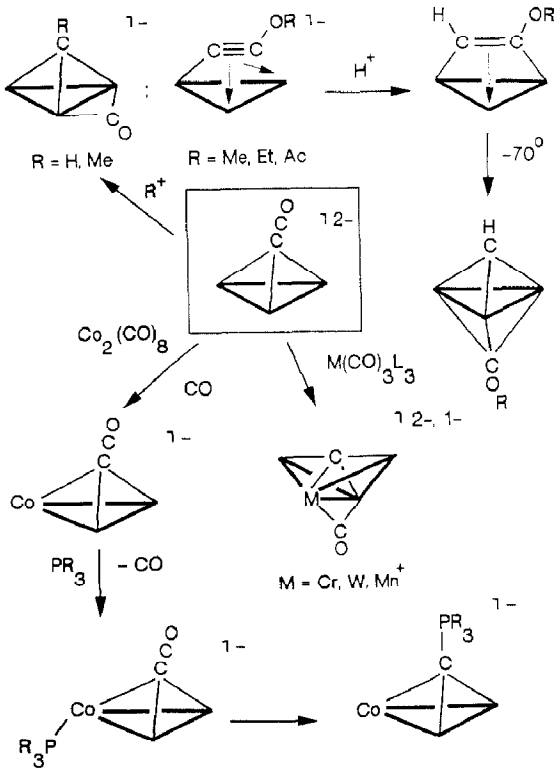


Scheme 1. Reactivity of the iron ketenylidene, $[Fe_3(CO)_9CCO]^{2-}$.

These include ligand transformations to form alkylidynes, acetylides and alkynes [3]; cluster building to give higher nuclearity mixed-metal carbide clusters [4]; and metal substitution to produce a mixed-metal ketenylidene [5], which undergoes reaction with phosphines to form ylide derivatives [6].

Protonation of the ketenylidene occurs at the $\alpha$ carbon ($\alpha$ indicates the primary carbon of the ligand, i.e., $\alpha C-\beta C-O$) with displacement of a carbonyl to the metal framework to give a methylidyne $[Fe_3(CO)_{10}CH]^-$. Methyl cation sources react analogously, to yield the alkylidyne cluster $[Fe_3(CO)_{10}CCH_3]^-$. In addition, methyl triflate also attacks the ketenylidene oxygen atom to form an acetylide $[Fe_3(CO)_9CCOCH_3]^-$ in a 1/2 ratio with the alkylidyne at room temperature. Bulkier alkyl cation sources such as acetyl chloride and ethyl triflate produce only acetylides $[Fe_3(CO)_9CCOR]^-$ (Ia,Ib). When protonated at low temperatures, these acetylides form alkyne clusters $[Fe_3(CO)_9HCCOR]$. As the solution is warmed, the carbon–carbon triple bond cleaves at approximately $-70\,^{\circ}C$ and dialkylidyne clusters are formed.

The ketenylidene also reacts with a wide variety of metal complexes, which contain labile ligands, to give higher nuclearity carbide clusters. $[Mn(CO)_3(NCCH_3)_3]^+$ adds to yield $[Fe_3Mn(CO)_{13}C]^-$. One or two equivalents of $Cr(CO)_3(NCCH_3)_3$ afford $[Fe_3Cr(CO)_{13}C]^{2-}$ and $[Fe_3Cr_2(CO)_{13}C]^{2-}$. The analogous reaction with $W(CO)_3(NCCH_2CH_3)_3$ gives $[Fe_3W(CO)_{13}C]^{2-}$. $[Ni_3Fe_3(CO)_{13}C]^{2-}$ can be synthesized from the ketenylidene and three equivalents of $[CpNi(CO)]_2$. $[RhFe_3(CO)_{12}C]^-$, $[Rh_2Fe(CO)_{14}C]$, and $[Rh_3Fe_3(CO)_{15}C]^-$ can be formed sequentially by addition of appropriate rhodium carbonyl halide complexes.

In direct contrast to these cluster-building reactions, $Co_2(CO)_8$ reacts with the ketenylidene under a CO atmosphere in THF solution to produce a mixed-metal ketenylidene $[Fe_2Co(CO)_9CCO]^-$. Substitution of phosphine for a carbonyl ligand readily occurs at the cobalt atom. Most phosphine ligands then undergo migration onto the capping carbon to form ylide clusters $[Fe_2Co(CO)_9CPR_3]^-$.

We now report on the chemistry of two acetylide clusters $(PPN)[Fe_3(CO)_9CCOCH_2CH_3]$ (**Ia**) and $(PPN)[Fe_3(CO)_9CCOC(O)CH_3]$ (**Ib**), obtained by attack of bulky carbocations on the ketenylidene oxygen atom. These acetylides react with nucleophiles such as phosphines to yield unusual products.

## Experimental

All manipulations were performed using standard Schlenk techniques [7] or in a Vacuum/Atmospheres drybox under an atmosphere of prepurified nitrogen. Solvents were collected and stored under nitrogen after distillation from appropriate drying agents. Deuterated solvents (Aldrich) for NMR spectroscopy were also distilled from appropriate drying agents. Triflic acid (Aldrich) was distilled before use. Tertiary phosphines (Aldrich) were distilled prior to use if liquid; otherwise they were recrystallized.

Solution IR spectra were recorded on a Matteson Alpha Centauri benchtop FTIR at 2 $cm^{-1}$ resolution using 0.1 mm pathlength $CaF_2$ window cells. NMR spectra (Table 1) were recorded on JEOL FX-270 (1H, 269.65 MHz; $^{13}C$, 67.80 MHz; $^{31}P$, 109.16 MHz) or Varian XLA-400 ($^1H$, 400 MHz; $^{13}C$, 101 MHz; $^{31}P$, 162 MHz) spectrometers. $^{13}C$ spectra were recorded with $Cr(acac)_3$ present as a shiftless relaxation agent. $^1H$ and $^{13}C$ chemical shifts were reported positive if downfield from TMS, and were internally referenced to solvent. $^{31}P$ spectra were referenced to external 85% $H_3PO_4$ in $D_2O$. The FAB mass spectrum of $[Fe_3(CO)_9CCPMePh_2]$ was recorded by Dr. D.L. Hung of the Northwestern University Analytical Services Laboratory on a Hewlett–Packard HP5905A spectrometer. Elemental analyses were performed by Elbach Analytical Laboratories, Engelskirchen, West Germany.

The syntheses of $(PPN)[Fe_3(CO)_9CCOC(O)CH_3]$ and $(PPN)[Fe_3(CO)_9CCOCH_2CH_3]$ are in the literature [3]. (PPN)Cl (Alfa) and $Fe_3(CO)_{12}$ (Strem) were used as received.

Table 1a

$^1H$ NMR data for Ia, Ib, II, III [a,b,c]

| Compound | Chemical shifts (ppm) |
|---|---|
| $(PPN)[Fe_3(CO)_9CCOCH_2CH_3]$ (Ia) [d] | 4.18 (q, $J$(HH) 7.1 Hz); 1.43 (t, $J$(HH) 7.1 Hz) |
| $(PPN)[Fe_3(CO)_9CCOC(O)CH_3]$ (Ib) [d] | 2.30 |
| $(PPN)[Fe_3(CO)_9(PMePh_2)CCOCH_2CH_3]$ (II) [e] | 3.35 (q, $J$(HH) 7.2 Hz); 2.11 (d, $^2J$(PH) 12.4 Hz); 0.71 (t, $J$(HH) 6.8 Hz). |
| $[Fe_3(CO)_9CCPMePh_2]$ (III) | 7.90(q), 7.77(t), 7.68(m); 2.63 (d, $^2J$(PH) 13.2 Hz). |

[a] $CD_2Cl_2$ solution, room temperature. [b] Resonances due to PPN cation not reported. [c] d, doublet; t, triplet; q, quartet; m, multiplet. [d] as reported in ref. 3. [e] Phenyl resonances due to $PMePh_2$ overlap PPN cation, and are not reported.

Table 1b

$^{13}C$ $\{^1H\}$ NMR data for Ia, Ib, II, III [a,b,c]

| Compound | Chemical shifts (ppm) | $J(CC)$ (Hz) |
|---|---|---|
| Ia [d] | 217.1(CO); 160.7 (sd, αC); 148.5 (sd, βC). | 42 |
| Ib [d] | 216.1(CO); 172.9 (sd, αC); 132.2 (sd, βC). | 39 |
| II | 222.2 (br, 6CO); 219.7 (dd, br, βC, $^2J$(CP) 8 Hz);21 218.1 (br, 3CO); 88.6 (sd, br, αC). | 21 |
| III | 226.5 (dd, αC, $^2J$(CP) 4 Hz); 214.0 (6CO); 213.3 (3 CO); 68.2 (dd, βC, $J$(CP) 108 Hz). | 30 |

[a] $CD_2Cl_2$ solution, room temperature. [b] $^{13}C$ enriched at all reported carbons; alkyl and PPN cations not reported. [c] sd, satellite doublet on singlet; dd, satellite doublets on doublet; br, broad. [d] As reported in ref. 3.

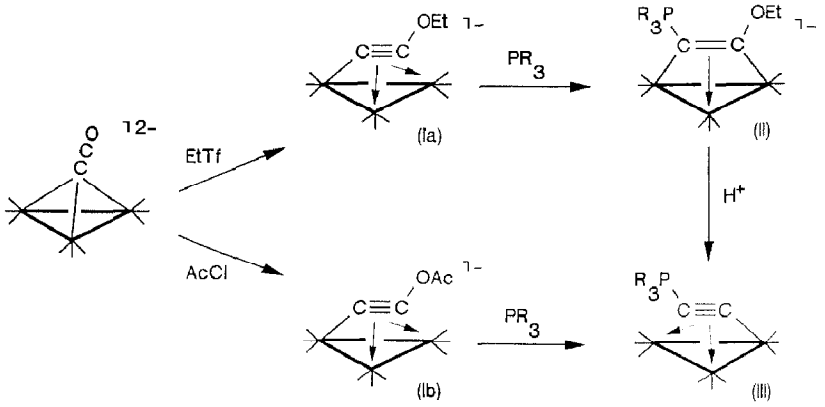


Scheme 2. Conversion of clusters Ia, Ib to II and III.

*Synthesis of (PPN)[$Fe_3(CO)_9(PMePh_2)CCOCH_2CH_3$) (II) (Scheme 2)*

A 390 mg (0.38 mmol) sample of (PPN)[$Fe_3(CO)_9CCOCH_2CH_3$] (Ia) was dissolved $CH_2Cl_2$ in 10 ml $CH_2Cl_2$. 170 μl (0.91 mmol) $PMePh_2$ was added and the solution was stirred for 0.5 h. After evaporation of the solution under vacuum removed excess phosphine, the red-violet solid was redissolved in 10 ml $CH_2Cl_2$ and 15 ml i-PrOH. Slow evaporation of the solution under vacuum afforded black-purple crystalline needles. The product was isolated by filtration and washed with pentane prior to vacuum drying. Yield: 410 mg, 88%. Anal. Found: Fe, 13.75; P, 7.63; C, 60.73; H, 3.83. $Fe_3P_3O_{10}NC_{62}H_{48}$ calcd.: Fe, 13.65; P, 7.57; C, 60.67; H, 3.94%. IR (2200 to 1500 $cm^{-1}$, $CH_2Cl_2$): 2009m; 1946vs; 1935vs; 1885w. $^{31}P$ $\{^1H\}$ NMR ($CD_2Cl_2$, +20 °C): +19.5 ppm, ($PPN^+$ not reported).

*Synthesis of [$Fe_3(CO)_9CCPMePh_2$] (III)*

A 490 mg (0.47 mmol) sample of (PPN)[$Fe_3(CO)_9CCOC(O)CH_3$] was dissolved in 10 ml $CH_2Cl_2$. 220 μl (1.18 mmol) $PMePh_2$ was added. After stirring for 0.5 h, the solution was evaporated to remove excess phosphine. The oily red-brown solids were redissolved in 10 ml $CH_2Cl_2$ and 15 ml i-PrOH. Slow evaporation under vacuum produced red microcrystals. After cooling in a 0 °C freezer to ensure maximum precipitation, the product was collected by filtration and washed with

isopropanol and pentane before vacuum drying. Yield: 180 mg, 59%. Anal. Found: C, 44.66; H, 2.13; P, 4.88. $Fe_3PO_9C_{24}H_{13}$ calcd.: C, 44.77; H, 2.04; P, 4.81%. IR (2200 to 1500 $cm^{-1}$, $CH_2Cl_2$): 2063m; 2010vs; 2001vs; 1988s,sh; 1573w. $^{31}P$ $\{^1H\}$ NMR ($CD_2Cl_2$, +20°C): +28.5 ppm. Mass spectrum: parent ion *m/e* 643, followed by successive loss of six carbonyls; then *m/e* 225.

*X-ray crystal structure determination of (PPN)[$Fe_3(CO)_9PMePh_2CCOEt$] (II)*

A dark red crystal of II suitable for X-ray diffraction was grown by slow diffusion of pentane into a $CH_2Cl_2$ solution of the cluster. The crystal was mounted in air on a glass fiber and transferred to the cold (−120°C) stream of an Enraf–Nonius CAD4 diffractometer. A summary of the data collection is given in Table 2. Unit cell parameters were determined by least-squares refinement on the setting angles of 25 unique reflections. The data were corrected for Lorentz and polarization effects. Four standard reflections were monitored every 3 h throughout the data collection and showed no loss of intensity, so a decay correction was not applied. Absorption corrections were made by the program DIFABS [8]. The transmission factors ranged from 0.91 to 1.25.

All calculations were done using the TEXSAN 4.0 software package [9a] run on a MicroVAX 3600 computer equipped with 32 MB physical memory and a 2 GB disk system. The structure was determined by direct methods (SHELXS 86) [10] and difference Fourier techniques. Inspection of initial difference maps indicated dis-

Table 2

Crystal data for (PPN)[$Fe_3(CO)_9PMePh_2CCOEt$] (II)

| | |
|---|---|
| Formula | $Fe_3O_{10}P_3C_{62}H_{48}N$ |
| *M* | 1227.52 |
| Crystal size, mm | 0.47×0.48×0.10 |
| Crystal system | triclinic |
| Space group | $P\bar{1}$ |
| *a*, Å | 9.910(1) |
| *b*, Å | 16.920(2) |
| *c*, Å | 17.372(2) |
| *α*, deg | 74.83(1) |
| *β*, deg | 84.65(1) |
| γ, deg | 86.07(1) |
| *V*, $Å^3$ | 2796(1) |
| *Z* | 2 |
| *d* (calc), g $cm^{-3}$ | 1.46 |
| *μ* (Mo-$K_\alpha$), $cm^{-1}$ | 9.10 |
| Radiation | Mo-$K_\alpha$ (λ 0.71069 Å), graphite-monochromated |
| Scan type | $\omega$–$2\theta$ |
| $2\theta$ range, deg | 4–50 |
| Unique data | 7742 |
| Unique data, $I > 3\sigma(I)$ | 6448 |
| No. of parameters | 542 |
| $R(F)$ | 0.042 |
| $R_w(f)$ | 0.065 |
| GOF | 1.68 |

Table 3

Crystal data for $[Fe_3(CO)_9CCPMePh_2]$ (III)

| | |
|---|---|
| Formula | $C_{24}H_{13}Fe_3O_9P$ |
| *M* | 643.88 |
| Crystal size, mm | $0.1 \times 0.3 \times 0.3$ |
| Crystal system | Orthorhombic |
| Space group | *Pbca* (No. 61) |
| *a*, Å | 7.898(1) |
| *b*, Å | 19.885(2) |
| *c*, Å | 31.906(5) |
| *V*, Å$^3$ | 5011(2) |
| *Z* | 8 |
| *d* (calc), g cm$^{-3}$ | 1.71 |
| $\mu$ (Mo-$K_\alpha$), cm$^{-1}$ | 18.2 |
| Radiation | Mo-$K_\alpha$ ($\lambda$ 0.71069 Å), graphite-monochromated |
| Scan type | $\omega$ |
| $2\theta$ range, deg. | 4–50 |
| Unique data | 5002 |
| Unique data, $I > 3\sigma(I)$ | 2606 |
| No. of parameters | 334 |
| $R(F)$ | 0.035 |
| $R_w(F)$ | 0.041 |
| GOF | 1.022 |

Table 4

Selected bond distances (Å) and angles (deg) with standard deviations for (PPN)$[Fe_3(CO)_9PMePh_2$-CCOEt] (II)

| Bond distances | | | | Bond angles | | | |
|---|---|---|---|---|---|---|---|
| Fe1–Fe2 | 2.5628(8) | C56–C51 | 1.396(6) | Fe1–Fe2–Fe3 | 57.84(2) | O1–C3–C4B | 114.8(9) |
| Fe1–Fe3 | 2.5317(8) | C2–O1 | 1.386(5) | Fe2–Fe1–Fe3 | 63.19(2) | C4A–C3–C4B | 79.0(9) |
| Fe2–Fe3 | 2.6691(8) | O1–C3 | 1.455(6) | Fe1–Fe3–Fe2 | 58.98(2) | C1–P1–C41 | 110.5(2) |
| C1–Fe1 | 2.034(4) | C3–C4A | 1.30(1) | Fe1–C11–O11 | 179.3(4) | C1–P1–C51 | 116.5(2) |
| C1–Fe3 | 1.986(4) | C3–C4B | 1.33(1) | Fe1–C12–O12 | 172.9(4) | C1–P1–C61 | 112.5(2) |
| C2–Fe1 | 2.128(4) | C4A–C4B | 1.67(2) | Fe1–C13–O13 | 177.7(4) | C41–P1–C51 | 105.7(2) |
| C2–Fe2 | 1.929(4) | Fe1–C11 | 1.770(4) | Fe2–C21–O21 | 176.1(4) | C41–P1–C61 | 105.3(2) |
| C1–C2 | 1.393(5) | Fe1–C12 | 1.777(4) | Fe2–C22–O22 | 175.9(4) | C51–P1–C61 | 105.4(2) |
| C1–P1 | 1.758(4) | Fe1–C13 | 1.773(4) | Fe2–C23–O23 | 178.3(4) | C46–C41–C42 | 119.7(4) |
| P1–C41 | 1.809(4) | Fe2–C21 | 1.765(5) | Fe3–C31–O31 | 175.7(3) | C41–C42–C43 | 120.5(4) |
| P1–C51 | 1.815(4) | Fe2–C22 | 1.798(4) | Fe3–C32–O32 | 178.2(3) | C42–C43–C44 | 119.5(4) |
| P1–C61 | 1.802(4) | Fe2–C23 | 1.754(4) | Fe3–C33–O33 | 174.2(3) | C43–C44–C45 | 120.0(4) |
| C41–C42 | 1.394(5) | Fe3–C31 | 1.783(4) | Fe2–C2–C1 | 110.8(3) | C44–C45–C46 | 121.0(4) |
| C42–C43 | 1.389(6) | Fe3–C32 | 1.766(4) | Fe3–C1–C2 | 107.1(3) | C45–C46–C41 | 119.3(4) |
| C43–C44 | 1.397(6) | Fe3–C33 | 1.778(4) | Fe1–C1–C2 | 74.1(2) | C56–C51–C52 | 119.3(4) |
| C44–C45 | 1.373(6) | C11–O11 | 1.157(5) | Fe1–C2–C1 | 66.9(2) | C51–C52–C53 | 119.6(4) |
| C45–C46 | 1.396(6) | C12–O12 | 1.151(5) | C1–C2–O1 | 116.4(3) | C52–C53–C54 | 120.6(4) |
| C46 C41 | 1.394(6) | C13–O13 | 1.146(5) | C2–C1–P1 | 121.2(3) | C53–C54–C55 | 120.1(4) |
| C51–C52 | 1.395(6) | C21–O21 | 1.164(5) | C2–O1–C3 | 119.1(3) | C54–C55–C56 | 120.2(4) |
| C52–C53 | 1.388(6) | C22–O22 | 1.147(5) | O1–C3–C4A | 117.4(7) | C55–C56–C51 | 120.1(4) |
| C53–C54 | 1.380(7) | C23–O23 | 1.160(5) | | | | |
| C54–C55 | 1.372(7) | C31–O31 | 1.151(5) | | | | |
| C55–56 | 1.388(6) | C32–O32 | 1.159(5) | | | | |
| | | C33–O33 | 1.154(5) | | | | |

Table 5

Positional parameters for (PPN)[$Fe_3(CO)_9PMePh_2CCOEt$] (II)

| Atom | $x$ | $y$ | $z$ |
|---|---|---|---|
| Fe1 | 0.22802(5) | 0.24822(3) | 0.23957(3) |
| Fe2 | −0.01838(5) | 0.29405(3) | 0.27060(3) |
| Fe3 | 0.14825(5) | 0.23035(3) | 0.38560(3) |
| P1 | 0.3739(1) | 0.38016(6) | 0.31630(6) |
| O1 | 0.1576(3) | 0.4406(2) | 0.2084(2) |
| O11 | 0.2933(3) | 0.3213(2) | 0.0690(2) |
| O12 | 0.0853(3) | 0.1048(2) | 0.2332(2) |
| O13 | 0.4802(3) | 0.1513(2) | 0.2757(2) |
| O21 | −0.0864(4) | 0.3262(2) | 0.1045(2) |
| O22 | −0.2052(3) | 0.1590(2) | 0.3250(2) |
| O23 | −0.1815(3) | 0.4123(2) | 0.3392(2) |
| O31 | 0.0233(3) | 0.0710(2) | 0.4292(2) |
| O32 | −0.0209(3) | 0.3051(2) | 0.4972(2) |
| O33 | 0.3617(3) | 0.1529(2) | 0.4900(2) |
| C1 | 0.2306(4) | 0.3273(2) | 0.3097(2) |
| C2 | 0.1364(4) | 0.3614(2) | 0.2541(2) |
| C3 | 0.0879(7) | 0.4715(4) | 0.1356(4) |
| C4A | 0.125(1) | 0.5408(7) | 0.0883(6) |
| C4B | −0.022(1) | 0.5192(8) | 0.1429(9) |
| C11 | 0.2683(4) | 0.2923(2) | 0.1365(2) |
| C12 | 0.1338(4) | 0.1634(3) | 0.2372(2) |
| C13 | 0.3822(4) | 0.1906(3) | 0.2620(2) |
| C21 | −0.0620(4) | 0.3158(3) | 0.1708(3) |
| C22 | −0.1286(4) | 0.2096(3) | 0.3047(2) |
| C23 | −0.1169(4) | 0.3644(3) | 0.3129(3) |
| C31 | 0.0698(4) | 0.1343(2) | 0.4095(2) |
| C32 | 0.0455(4) | 0.2765(2) | 0.4520(2) |
| C33 | 0.2824(4) | 0.1862(2) | 0.4466(2) |
| C41 | 0.3284(4) | 0.4570(2) | 0.3708(2) |
| C42 | 0.4304(4) | 0.4977(2) | 0.3927(2) |
| C43 | 0.3980(5) | 0.5560(3) | 0.4356(2) |
| C44 | 0.2620(5) | 0.5734(2) | 0.4572(2) |
| C45 | 0.1616(4) | 0.5344(2) | 0.4345(3) |
| C46 | 0.1929(4) | 0.4756(2) | 0.3913(2) |
| C51 | 0.4606(4) | 0.4338(2) | 0.2224(2) |
| C52 | 0.4341(4) | 0.5174(3) | 0.1901(2) |
| C53 | 0.5012(5) | 0.5566(3) | 0.1179(3) |
| C54 | 0.5921(5) | 0.5135(3) | 0.0772(3) |
| C55 | 0.6186(5) | 0.4313(3) | 0.1086(3) |
| C56 | 0.5527(4) | 0.3907(3) | 0.1807(3) |
| C61 | 0.5024(4) | 0.3141(2) | 0.3709(2) |
| P2 | −0.5204(1) | −0.17965(6) | 0.25701(6) |
| P3 | −0.3174(1) | −0.06362(6) | 0.16158(6) |
| N | −0.4544(3) | −0.1099(2) | 0.1876(2) |
| C111 | −0.6552(4) | −0.2184(2) | 0.2161(2) |
| C112 | −0.7252(4) | −0.2850(3) | 0.2606(2) |
| C113 | −0.8310(5) | −0.3122(3) | 0.2303(3) |
| C114 | −0.8701(5) | −0.2720(3) | 0.1558(3) |
| C115 | −0.8016(5) | −0.2056(3) | 0.1107(3) |
| C116 | −0.6928(4) | −0.1786(3) | 0.1405(3) |
| C121 | −0.4060(4) | −0.2653(2) | 0.2959(2) |
| C122 | −0.3861(4) | −0.3283(2) | 0.2578(2) |
| C123 | −0.2908(4) | −0.3918(3) | 0.2824(3) |

Table 5 (continued)

| Atom | x | y | z |
|---|---|---|---|
| C124 | −0.2162(5) | −0.3921(3) | 0.3459(3) |
| C125 | −0.2356(5) | −0.3301(3) | 0.3838(3) |
| C126 | −0.3305(4) | −0.2650(3) | 0.3587(3) |
| C131 | −0.5936(4) | −0.1416(2) | 0.3398(2) |
| C132 | −0.6400(4) | −0.1954(3) | 0.4118(2) |
| C133 | −0.6982(4) | −0.1658(3) | 0.4735(3) |
| C134 | −0.7132(5) | −0.0825(3) | 0.4653(3) |
| C135 | −0.6698(5) | −0.0285(3) | 0.3938(3) |
| C136 | −0.6112(4) | −0.0584(3) | 0.3312(3) |
| C141 | −0.2273(4) | −0.0983(2) | 0.0801(2) |
| C142 | −0.2110(4) | −0.1820(2) | 0.0874(2) |
| C143 | −0.1412(4) | −0.2120(3) | 0.0274(3) |
| C144 | −0.0884(5) | −0.1574(3) | −0.0412(3) |
| C145 | −0.1056(5) | −0.0744(3) | −0.0493(3) |
| C146 | −0.1743(4) | −0.0444(3) | 0.0113(3) |
| C151 | −0.2036(4) | −0.0752(2) | 0.2389(2) |
| C152 | −0.0797(5) | −0.1171(3) | 0.2363(3) |
| C153 | 0.0022(5) | −0.1279(3) | 0.2986(3) |
| C154 | −0.0358(5) | −0.0936(3) | 0.3620(3) |
| C155 | −0.1580(4) | −0.0508(3) | 0.3636(3) |
| C156 | −0.2424(4) | −0.0420(3) | 0.3034(2) |
| C161 | −0.3597(4) | 0.0439(2) | 0.1251(2) |
| C162 | −0.2727(4) | 0.1024(3) | 0.1312(2) |
| C163 | −0.3079(5) | 0.1852(3) | 0.1002(3) |
| C164 | −0.4281(5) | 0.2086(3) | 0.0654(3) |
| C165 | −0.5153(5) | 0.1501(3) | 0.0601(3) |
| C166 | −0.4809(4) | 0.0678(3) | 0.0897(2) |

order of the terminal methyl carbon of the ethoxide substituent between two sites, C4A and C4B. The disorder was resolved by placing carbon atoms in both sites with 50% occupancy. Least-squares refinement was performed initially with isotropic thermal parameters, and then with anisotropic parameters for all atoms except PPN cation carbons and all hydrogens. Hydrogen atoms were located on a difference Fourier map and introduced without refinement into the calculations, except for those on the ethoxide carbons. The largest peak in the final difference map was 0.76 e/Å$^3$ high. The final positional parameters are given in Table 5, and relevant bond distances and angles in Table 4.

*X-ray crystal structure determination of [$Fe_3(CO)_9CCPMePh_2$] (III)*

A red crystal of III suitable for X-ray diffraction was grown by slow diffusion of pentane into a $CH_2Cl_2$ solution of the cluster. The crystal was mounted on a glass fiber in air and transferred to the cold (−120°C) stream of an Enraf–Nonius CAD4 diffractometer. A summary of the data collection is given in Table 3. Preliminary measurements indicated an orthorhombic unit cell, and the space-group *Pbca* (No. 61) was uniquely assigned on the basis of systematic absences. Unit cell parameters were determined by least-squares refinement of the setting angles of 25 unique reflections. The intensities of four standard reflections were monitored every 3 h. No loss of intensity was observed and a decay correction was not applied. The

Table 6

Selected bond distances (Å) and angles (deg) with standard deviations for $[Fe_3(CO)_9CCPMePh_2]$ (III)

| Bond distances | | | | Bond angles | | | |
|---|---|---|---|---|---|---|---|
| Fe1–Fe2 | 2.496(1) | Fe1–C1 | 1.773(6) | Fe1–Fe2–Fe3 | 62.23(3) | C26–C21–C22 | 119.6(5) |
| Fe1–Fe3 | 2.661(1) | Fe1–C2 | 1.782(5) | Fe2–Fe1–Fe3 | 61.69(3) | C21–C22–C23 | 119.8(5) |
| Fe2–Fe3 | 2.648(1) | Fe1–C3 | 1.784(6) | Fe1–Fe3–Fe2 | 56.08(3) | C22–C23–C24 | 120.2(5) |
| C10–Fe1 | 2.023(5) | Fe2–C4 | 1.804(6) | Fe1–C1–O1 | 178.2(5) | C23–C24–C25 | 120.5(5) |
| C10–Fe2 | 2.010(5) | Fe2–C5 | 1.773(6) | Fe1–C2–O2 | 175.6(5) | C24–C25–C26 | 120.0(5) |
| C10–Fe3 | 1.790(5) | Fe2–C6 | 1.770(6) | Fe1–C3–O3 | 177.1(6) | C25–C26–C21 | 119.9(5) |
| C11–Fe1 | 2.066(5) | Fe3–C7 | 1.809(6) | Fe2–C4–O4 | 179.6(7) | C36–C31–C32 | 119.6(5) |
| C11–Fe2 | 2.078(5) | Fe3–C8 | 1.772(6) | Fe2–C5–O5 | 177.4(6) | C31–C32–C33 | 120.0(5) |
| C10–C11 | 1.310(7) | Fe3–C9 | 1.763(6) | Fe2–C6–O6 | 175.4(6) | C32–C33–C34 | 119.4(5) |
| C11–P | 1.735(5) | C1–O1 | 1.149(6) | Fe3–C7–O7 | 179.5(6) | C33–C34–C35 | 121.0(5) |
| P–C12 | 1.790(5) | C2–O2 | 1.144(6) | Fe3–C8–O8 | 178.8(5) | C34–C35–C36 | 120.2(5) |
| P–C21 | 1.789(5) | C3–O3 | 1.150(7) | Fe3–C9–O9 | 178.2(6) | C35–C36–C31 | 119.8(5) |
| P–C31 | 1.786(5) | C4–O4 | 1.144(7) | Fe3–C10–C11 | 156.7(4) | | |
| C21–C22 | 1.408(7) | C5–O5 | 1.150(7) | C10–C11–P | 142.4(4) | | |
| C22–C23 | 1.376(8) | C6–O6 | 1.149(7) | C11–P–C12 | 110.3(2) | | |
| C23–C24 | 1.386(8) | C7–O7 | 1.151(6) | C11–P–C21 | 111.7(2) | | |
| C24–C25 | 1.381(8) | C8–O8 | 1.139(7) | C11–P–C31 | 109.4(2) | | |
| C25–C26 | 1.388(7) | C9–O9 | 1.142(7) | C12–P–C21 | 108.7(2) | | |
| C26–C21 | 1.391(7) | | | C12–P–C31 | 109.8(2) | | |
| C31–C32 | 1.393(7) | | | C21–P–C31 | 107.0(2) | | |
| C32–C33 | 1.394(7) | | | | | | |
| C33–C34 | 1.366(8) | | | | | | |
| C34–C35 | 1.382(8) | | | | | | |
| C35–C36 | 1.375(7) | | | | | | |
| C36–C31 | 1.390(7) | | | | | | |

data were corrected for Lorentz and polarization effects. Absorption corrections were done using the program DIFABS [8]. The transmission factors ranged from 0.80 to 1.18.

All calculations were done using the TEXSAN 2.0 software package [9b]. The structure was determined by direct methods (SHELXS 86) [10] and difference Fourier techniques. Least-squares refinement was performed initially with isotropic thermal parameters, and then with anisotropic parameters for all non-hydrogen atoms. All hydrogen atoms were located on a difference Fourier map and introduced into the calculations without refinement. The largest peak in the final difference map was 0.348 e/Å$^3$ high. The final positional parameters are given in Table 7, and relevant bond distances and angles in Table 6.

## Results and discussion

Coordination to an ensemble of metals can impart unusual, interesting, and potentially important reactivity to organic substrates [2], the nature of which is influenced both by the bonding mode [2] and the identity of the metals [11]. In particular the reactivity of acetylide clusters has attracted considerable attention [12]. A large number of acetylide clusters have been prepared with the acetylide coordinated in a variety of fashions [12,13,14]. Although monometallic acetylide

Table 7

Positional parameters for $[Fe_3(CO)_9CCPMePh_2]$ (III)

| Atom | x | y | z |
|---|---|---|---|
| Fe1 | 0.0617(1) | −0.07748(3) | 0.41702(2) |
| Fe2 | 0.1132(1) | −0.05665(4) | 0.34093(2) |
| Fe3 | −0.1549(1) | −0.12924(4) | 0.36186(2) |
| P | −0.0030(2) | 0.09416(6) | 0.38738(4) |
| O1 | −0.1463(6) | −0.0826(3) | 0.4931(1) |
| O2 | 0.1964(5) | −0.2142(2) | 0.4225(1) |
| O3 | 0.3770(6) | −0.0199(2) | 0.4487(1) |
| O4 | 0.0118(8) | −0.0081(2) | 0.2573(1) |
| O5 | 0.4505(6) | 0.0033(2) | 0.3453(2) |
| O6 | 0.2460(6) | −0.1869(2) | 0.3146(1) |
| O7 | −0.0523(6) | −0.2722(2) | 0.3568(1) |
| O8 | −0.3183(8) | −0.1236(2) | 0.2801(2) |
| O9 | −0.4491(6) | −0.1491(2) | 0.4150(2) |
| C1 | −0.0649(8) | −0.0795(3) | 0.4633(2) |
| C2 | 0.1384(7) | −0.1617(3) | 0.4195(2) |
| C3 | 0.2510(8) | −0.0421(3) | 0.4372(2) |
| C4 | 0.0506(8) | −0.0269(3) | 0.2898(2) |
| C5 | 0.3165(8) | −0.0191(3) | 0.3430(2) |
| C6 | 0.1874(8) | −0.1368(3) | 0.3253(2) |
| C7 | −0.0928(8) | −0.2167(3) | 0.3587(2) |
| C8 | −0.254(1) | −0.1265(3) | 0.3121(2) |
| C9 | −0.3341(8) | −0.1422(3) | 0.3938(2) |
| C10 | −0.1027(7) | −0.0436(2) | 0.3732(1) |
| C11 | −0.0052(7) | 0.0072(2) | 0.3834(1) |
| C12 | 0.2052(6) | 0.1231(3) | 0.4001(2) |
| C21 | −0.1469(6) | 0.1235(2) | 0.4266(1) |
| C22 | −0.1316(7) | 0.1901(3) | 0.4410(2) |
| C23 | −0.2506(8) | 0.2158(3) | 0.4681(2) |
| C24 | −0.3830(8) | 0.1758(3) | 0.4820(2) |
| C25 | −0.3982(7) | 0.1102(3) | 0.4684(2) |
| C26 | −0.2818(7) | 0.0841(3) | 0.4402(2) |
| C31 | −0.0693(6) | 0.1300(2) | 0.3387(1) |
| C32 | 0.0021(7) | 0.1897(3) | 0.3242(2) |
| C33 | −0.0559(7) | 0.2185(3) | 0.2870(2) |
| C34 | −0.1842(8) | 0.1880(3) | 0.2655(2) |
| C35 | −0.2575(8) | 0.1294(3) | 0.2800(2) |
| C36 | −0.2003(7) | 0.1001(3) | 0.3164(2) |

complexes show expected nucleophilic behavior [15], addition of nucleophiles such as phosphines [12,16], phosphites [12], amines [12,17,18], methylenes [19], and alkoxides [18] to acetylide ligands of neutral and cationic clusters is well documented. We have extended this chemistry to monoanionic clusters, with unusual results.

*Reactions of (PPN)[$Fe_3(CO)_9CCOR$] (Ia,Ib) with $PMePh_2$*

When a solution of Ia is treated with $PMePh_2$, one equivalent of phosphine is added at the acetylide $\alpha$ carbon to give II in high yield. Therefore, II is formulated as a zwitterionic phosphonium alkyne cluster (eq. 2). The five electron donor

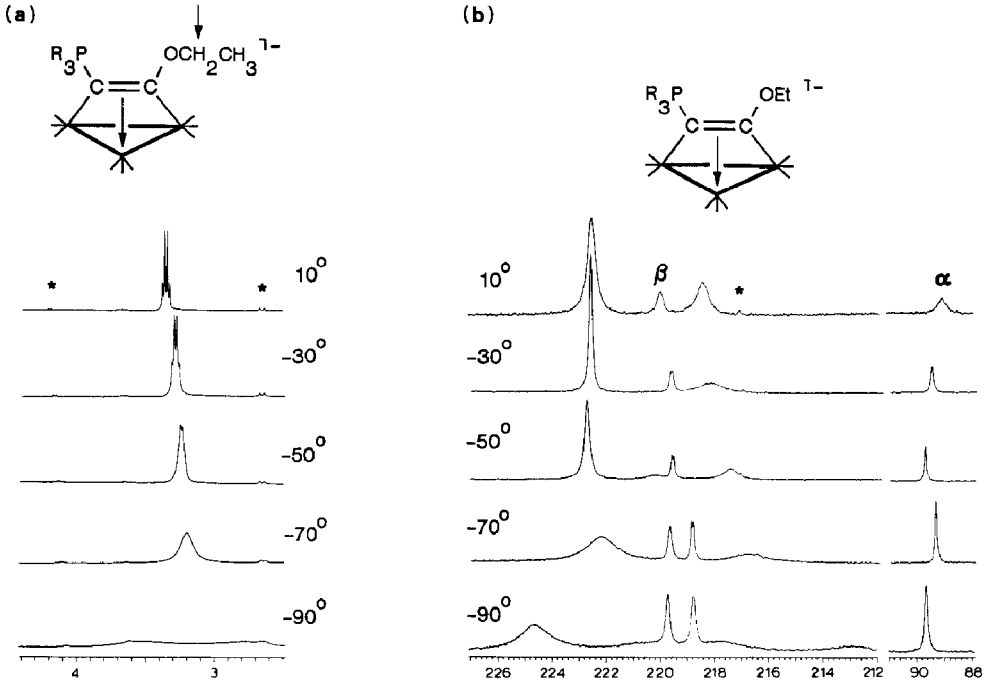


Fig. 1a. $^1H$ NMR resonance of the methylene protons on II in $CD_2Cl_2$ at various temperatures, indicating fluxionality of the alkyne. The scale is ppm downfield from TMS. Minor resonances marked with an asterisk are due to methylene protons of Ia and the methyl protons of free $PMePh_2$.

Fig. 1b. $^{13}C$ $\{^1H\}$ spectrum of II at various temperatures, reflecting fluxional behavior in solution. The scale is ppm downfield from TMS. The resonance labelled with an asterisk due to carbonyls of Ia.

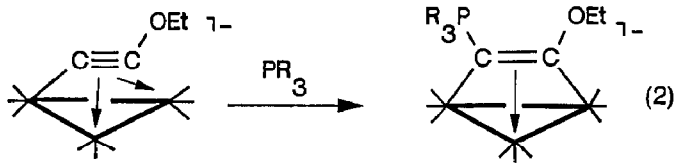


(1σ,4π)-acetylide becomes a four electron donor (2σ,2π)-alkyne, with the extra electron provided by formation of the phosphonium zwitterion. An X-ray crystal structure determination was performed on II and is discussed below.

As expected, the solution IR spectrum of II contains CO stretching frequencies that are on average 40 $cm^{-1}$ lower than those of Ia. The $^1H$ NMR resonances for the ethoxy protons occur substantially upfield in II compared to those of Ia, implying the phosphonium alkyne ligand is more electron rich than the acetylide. This might be accounted for by differing coordination modes or less than complete delocalization to the metal framework of the electron provided by the zwitterion.

Variable temperature NMR studies (Fig. 1) indicate that the behavior of II in solution is quite complex. The methylene protons of the ethoxide substituent are equivalent in the $^1H$ spectrum at room temperature. This clearly implies the existence of a dynamic mirror plane and interconversion of enantiomers by alkyne flipping [20]. At $-90\,°C$, the resonance broadens and splits into two resonances as this fluxionality is halted. The $^{31}P$ resonance of the phosphonium also becomes quite broad at the critical temperature.

The carbonyl ligands are involved in rapid intrametal fluxionality at room temperature. Thus two peaks in a 2/1 intensity ratio are seen, with six carbonyls on two iron atoms related by the dynamic mirror plane. The smaller resonance, corresponding to the carbonyl on the iron that is $\pi$-bonded to the alkyne, divides into two 2/1 resonances at $-50\,^{\circ}C$ as the carbonyls become rigid on that metal vertex. These peaks become sharper at $-60\,^{\circ}C$, but the larger resonance then broadens as mirror-plane symmetry is lost. The large resonance of six carbonyls also begins to broaden at $-60\,^{\circ}C$ as fluxionality is slowed, but the critical temperature lies near that of the alkyne flipping which, of course, affects this resonance also.

One would expect to see large coupling between the phosphorus atom and the $\alpha$ carbon of the alkyne to which it is bonded. Despite this seemingly reasonable expectation, no coupling to the $\alpha$ carbon is observed, although there is slight coupling to the $\beta$ carbon ($^2J$(CP) 8 Hz). The assignment of the $\alpha$ and $\beta$ carbon resonances was confirmed by preparation of II selectively labelled with $^{13}C$ at the $\beta$ carbon. Similarly, two cationic monotungsten phosphonium methylidyne ($L_nW{\equiv}CPMe_3$) complexes lack carbon–phosphorus coupling, but tungsten–phosphorus coupling is seen, perhaps analogous to the P–$\beta$C coupling of II [21].

Above $-30\,^{\circ}C$, the carbonyl and acetylide $^{13}C$ resonances broaden, and a small, sharp resonance appears at 217.6 ppm near room temperature. This resonance corresponds to the carbonyls of the parent acetylide Ia, indicating II is in rapid equilibrium with Ia and free phosphine at ambient temperatures. The room temperature $^{13}C$ resonances are sharpened by the presence of excess phosphine. The resonance of Ia grows to roughly 5–10% as large as the carbonyl resonances of II at $60\,^{\circ}C$ in THF-$d_8$. This is reversible, and the resonance of Ia is diminished on cooling to lower temperatures. Further work is necessary to define quantitatively this equilibrium.

The carbon–phosphorus bond of II appears short from X-ray data (1.758(4) Å), suggesting it should be a strong, stable interaction. The equilibrium between Ia and II indicates otherwise. One of the tungsten methylidyne complexes discussed above provides a precedent [21a]. The complex will reversibly add a second equivalent of phosphine to form a bis(phosphonium)carbene. Unless excess phosphine is added, an equilibrium between the two complexes is observed. As with II, both C–P bond distances are relatively short (1.75(2) and 1.77(1) Å). One can imagine bonding analogies between these tungsten complexes and the clusters Ia and II, although significant comparisons may be difficult to make. Nonetheless, the reactivities of the tungsten methylidyne and Ia with phosphine are similar, at least superficially.

In marked contrast, Ib and $PMePh_2$ react with loss of $(PPN)(OC(O)CH_3)$ to yield III. Preparation of III from a sample of Ib enriched with $^{13}C$ at the carbonyls and acetylide carbons revealed both carbon–carbon and carbon–phosphorus coupling of acetylide-like resonances in the $^{13}C$ NMR spectrum. The value of $J$(CP) is much greater for the $\beta$ carbon (108 Hz) than for the $\alpha$ carbon (4 Hz), leading us to formulate III as a zwitterionic phosphonium acetylide cluster, $[Fe_3(CO)_9CCPMePh_2]$. This configuration was confirmed by the X-ray structure determination described below.

Alkyl phosphonium salts are known [22], as are mononuclear phosphonium acetylides [23]. Attack on acetylides, described earlier, yields a variety of ligands, including phosphonium alkynes and vinylidenes. Phosphine addition has been reported for a mononuclear vinylidene [24] and a (postulated) ketenylidene [25].

Thus it is not surprising that phosphines should react at the acetylide ligand of Ib. However, loss of acetate from Ib to form an acetylide, rather than an alkyne or substituted vinylidene was unexpected. Even more interesting is the formation of III from II by addition of one equivalent of triflic acid, $HSO_3CF_3$. The product was obtained as microcrystals in good yield and identified by IR and NMR ($^1H$, $^{13}C$, $^{31}P$). In keeping with structure III, no hydride resonance was observed in the proton NMR spectrum as far upfield as $-50$ ppm.

This result raises the possibility that both Ia and Ib add phosphine at iron to form phosphonium alkynes, but that Ib then loses acetate anion to form the acetylide cluster III, eq. 3. Ethoxide anion would obviously be a much poorer

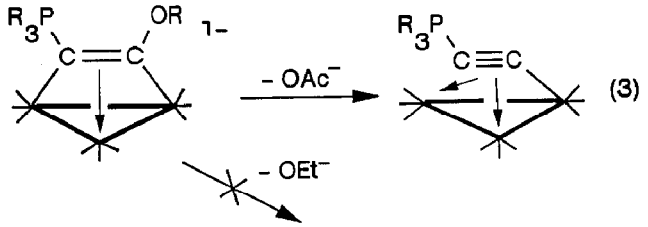


leaving group than acetate, preventing direct formation of III from Ia unless acid is present.

The reactions of both Ia and Ib with phosphine are rapid, and intermediates were not observed spectroscopically. To further elucidate the course of this reaction, samples of Ia and Ib enriched with $^{13}C$ at the carbonyls and acetylide $\beta$ carbons, but not the $\alpha$ carbons, were prepared. In situ monitoring of phosphine addition to Ib by $^{13}C$ NMR revealed the formation of III labelled exclusively at the carbonyls and at the acetylide carbon not bonded to phosphorus, eq. 4. Protonation of II gave an analogous result.

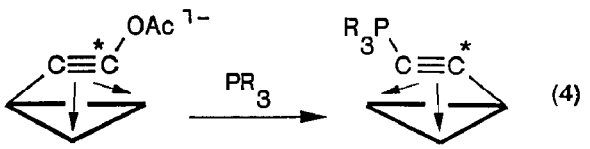


The phosphine in the resulting III was still bonded to the original $\alpha$ carbon, which was not bonded to the displaced ethoxide substituent. This experiment clearly rules out direct nucleophilic attack at the $\beta$ carbon of Ib and suggests the phosphine is rather added at the $\alpha$ carbon to form an unstable phosphonium alkyne similar to II. However, this does not disprove addition of a metal and subsequent migration to the ligand. Such a pathway has been unambiguously demonstrated with phosphines in a related system [6].

*X-ray crystal structure of (PPN)[$Fe_3(CO)_9PMePh_2CCOEt$] (II)*

An ORTEP representation of the cluster anion II is shown in Fig. 2. The structure of the PPN cation is unremarkable. The alkyne bond of the cluster lies parallel to an iron–iron bond, and has a fairly normal length of 1.393(5) Å [13]. Neutral triiron nonacarbonyl clusters typically display perpendicular alkyne bonding [26], but the monoanionic charge of II and the zwitterionic phosphonium alkyne

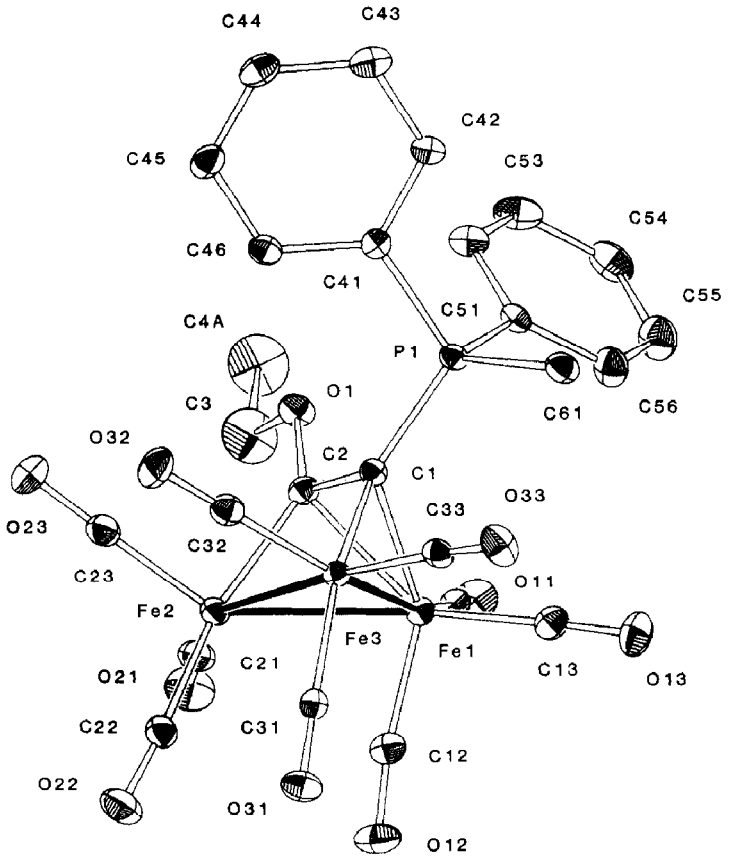


Fig. 2. An ORTEP drawing of the cluster anion $[Fe_3(CO)_9PMePh_2CCOEt)^-$ (II) with 30% probability ellipsoids. Only one orientation of the disordered ethoxide group is shown.

provide the extra two electrons theoretically necessary to stabilize a parallel configuration [27].

The alkyne substituents are bent away from the metal triangle at the fairly shallow angles of 116.4(3) degrees for the ethoxide (C$\alpha$–C$\beta$–O) and 121.2(3)° for the phosphonium (C$\beta$–C$\alpha$–P). However, these values are not atypical [13]. Bond angles about the phosphorus atom are slightly distorted from tetrahedral. As expected, the zwitterionic nature of the phosphine is reflected in the shortened C$\alpha$–P bond distance of 1.758(4) Å. The other three phosphorus–carbon bonds are slightly longer. The metal triangle is not perfectly equilateral. The iron–iron bond spanned by the alkyne is approximately 0.1 Å longer than the other two which differ only slightly.

*X-ray crystal structure of $[Fe_3(CO)_9CCPMePh_2]$ (III)*

As seen in Fig. 3 (III) has a structure typical of trimetallic acetylides [13]. The acetylide triple bond lies perpendicular to a metal–metal bond, in agreement with theoretical considerations [27]. This metal–metal bond is substantially shorter than the other two, which likely arises due to $4\pi$ coordination of the triple bond to the two iron centers. Relevant bond distances and angles are given in Table 6. Positional parameters are listed in Table 7. The acetylide C–C bond length, 1.310(7) Å, is typical of coordinated acetylides and alkynes, and is not significantly different

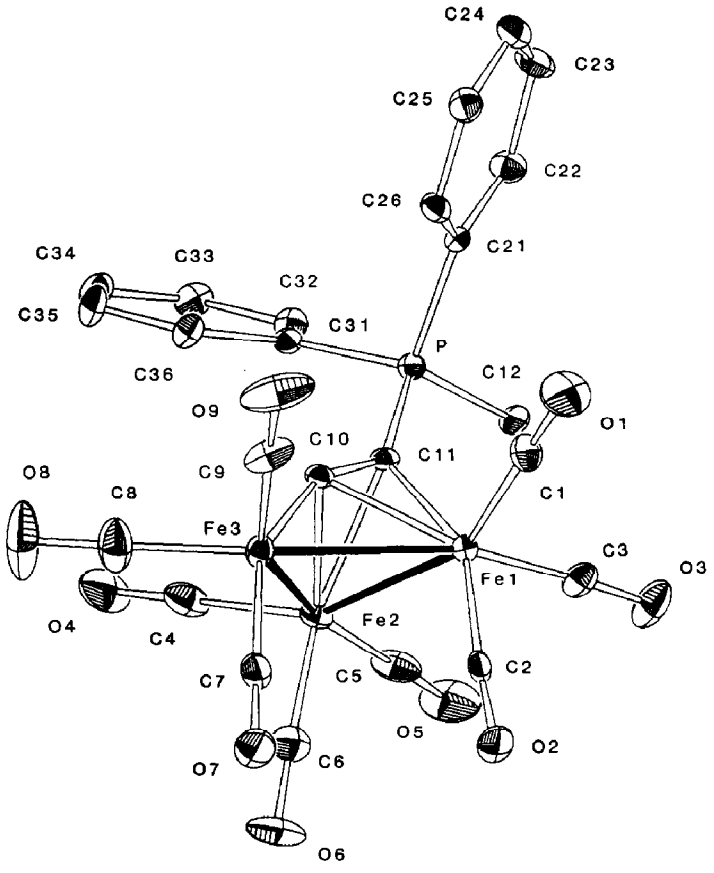


Fig. 3. An ORTEP diagram of $[Fe_3(CO)_9CCPMePh_2]$ (III) with thermal ellipsoids drawn at 35% probability.

from that of Ib [3]. Bond angles about the phosphorus atom are essentially tetrahedral. However, the bond to the acetylide $\beta$ carbon is significantly shorter than the other three, underscoring the zwitterionic nature of the acetylide. The $\alpha C-\beta C-P$ angle of 142.4(4) degrees is significantly bent from that seen for mononuclear phosphonium acetylides, which are approximately linear [23].

*Reactions of Ia,Ib with other nucleophiles*

The reactions of Ia and Ib with $PMePh_2$ appear general when extended to other tertiary phosphines and phosphites. Products of the reaction of Ia and Ib with $P(OMe)_3$, $PMe_3$, $PMe_2Ph$, $PPh_3$, and $PCy_3$ (Cy = cyclohexyl), have been generated in situ and appear similar in nature to II and III spectroscopically. Additionally, Ib undergoes reaction with t-butylisocyanide over the course of four days when present in a four-fold excess at room temperature. Characterization of these products is not yet complete. No reaction with triphenyl arsine was observed in solution at room temperature.

## Conclusions

Acetylide clusters Ia and Ib add one equivalent of tertiary phosphine despite their overall anionic charge. Analogies suggest that both add the phosphine at the $\alpha$

carbon to form an alkyne. With Ib this is followed by loss of the acetate group from C$\beta$ of the intermediate alkyne to form the observed phosphonium acetylide (III).

Acetylides such as Ia and Ib promise to open still more synthetic applications of the already diverse chemistry of the ketenylidene ligand.

## Acknowledgements

We thank a reviewer for useful comments concerning spectral data of II. This work has been supported by the NSF Synthetic Organometallic Program, grant CHE-8942133.

## References

1 S. Ching, J.A. Hriljac, M.J. Sailor, J.W. Kolis, M.P. Jensen, D.F. Shriver, Inorganic Syntheses, submitted.
2 D.F. Shriver, M.J. Sailor, Acc. Chem. Res., 21 (1988) 374.
3 J.A. Hriljac, D.F. Shriver, J. Am. Chem. Soc., 109 (1987) 6010.
4 J.A. Hriljac, S. Harris, D.F. Shriver, Inorg. Chem., 27 (1988) 816.
5 S. Ching, E.M. Holt, J.W. Kolis, D.F. Shriver, Organometallics, 7 (1988) 892.
6 S. Ching, M. Sabat, D.F. Shriver, Organometallics, 8 (1989) 1047.
7 D.F. Shriver, M.A. Drezdzon, Manipulation of Air-Sensitive Compounds, 2nd. edit., Wiley Interscience, New York, 1986.
8 N. Walker, D. Stuart, Acta Cryst. A, 39 (1983) 158.
9 (a) P.N. Swepston, TEXSAN, Version 4.0, the TEXRAY Structure Analysis Program Package, Molecular Structure Corporation, College Station, TX, 1987; (b) P.N. Swepston, TEXSAN, Version 2.0, ibid., 1986.
10 G.M. Sheldrick, SHELXS 86; A program for crystal structure determination, University of Goettingen, FRG, 1986.
11 For example: M.J. Went, M.J. Sailor, P.L. Bogdan, C.P. Brock, D.F. Shriver, J. Am. Chem. Soc., 109 (1987) 6023.
12 A.J. Carty, Pure Appl. Chem., 54 (1982) 113, and ref. therein.
13 E. Sappa, A. Tiripicchio, P. Braunstein, Chem. Rev., 83 (1983) 203; and ref. therein.
14 A.J. Deeming, Adv. Organometallic Chem., 26 (1986) 1; and ref. therein.
15 (a) K.R. Birdwhistell, J.L. Templeton, Organometallics, 4 (1985) 2062; and ref. therein. (b) A. Mayr, K.C. Schaefer, E.Y. Huang, J. Am. Chem. Soc., 106 (1984) 1517.
16 (a) K. Henrick, M. McPartlin, A.J. Deeming, S. Hasso, P. Manning, J. Chem. Soc. Dalton Trans., (1982) 899; (b) S.P. Deraniyagala, K.R. Grundy, Organometallics, 4 (1985) 424.
17 (a) G.N. Mott, A.J. Carty, Inorg. Chem., 22 (1983) 2726; (b) A.J. Deeming, S.E. Kabir, D. Nuel, N.I. Powell, Organometallics, 8 (1989) 717.
18 E. Boyar, A.J. Deeming, S.E. Kabir, J. Chem. Soc. Chem. Commun., (1986) 577.
19 D. Nucciarone, N.J. Taylor, A.J. Carty, Organometallics, 3 (1984) 177.
20 This has been demonstrated on a related system. E. Boyar, A.J. Deeming, M.S.B. Felix, S.E. Kabir, T. Adatia, R. Bhusate, M. McPartlin, H.R. Powell, J. Chem. Soc. Dalton Trans., (1989) 5.
21 (a) A.E. Bruce, A.S. Gamble, T.L. Tonker, J.L. Templeton, Organometallics, 6 (1987) 1350; (b) S.J. Holmes, R.R. Schrock, M.R. Churchill, H.J. Wasserman, Organometallics, 3 (1984) 476.
22 P. Cadiot, W. Chodkiewicz, in H.G. Viehe (Ed.), Chemistry of Acetylenes, Marcel Dekker, New York, 1969.
23 R.E. Cramer, K.T. Higa, J.W. Gilje, Organometallics, 4 (1985) 1140 and ref. therein.
24 D.R. Sem, A. Wong, A.T. Patton, M. Marsi, C.E. Strouse, J.A. Gladysz, J. Am. Chem. Soc., 110 (1988) 6096.
25 A.K. List, G.L. Hillhouse, A.L. Rheingold, J. Am. Chem. Soc., 110 (1988) 4855.
26 J.F. Blount, L.F. Dahl, C. Hoogzand, W. Hübel, J. Am. Chem. Soc., 88 (1966) 292.
27 D. Osella, R. Gobetto, P. Montangero, P. Zanello, A. Cinquantini, Organometallics, 5 (1986) 1247; and ref. therein.